

Reliable Wake-up Receiver with Increased Sensitivity using Low-Noise Amplifiers

Robert Fromm

Faculty of Engineering
Leipzig University of Applied Sciences
Leipzig, Germany
0000-0002-2905-0648

Olfa Kanoun

Department of Electrical Engineering
and Information Technology
Chemnitz University of Technology
Chemnitz, Germany
0000-0002-7166-1266

Fauzi Derbel

Faculty of Engineering
Leipzig University of Applied Sciences
Leipzig, Germany
0000-0002-7038-8157

Note: This is the manuscript version of this publication. See <https://doi.org/10.1109/SSD54932.2022.9955764> for the published version. Current version: July 24, 2025. ©2022 IEEE. Personal use of this material is permitted. Permission from IEEE must be obtained for all other uses, in any current or future media, including reprinting/republishing this material for advertising or promotional purposes, creating new collective works, for resale or redistribution to servers or lists, or reuse of any copyrighted component of this work in other works.

Abstract—For power-limited wireless sensor networks, energy efficiency is a critical concern. Receiving packages is proven to be one of the most power-consuming tasks of a wireless sensor node. To address this problem, the asynchronous communication is based on wake-up receivers. The proposed receiver circuit utilizes a two-stage low-noise amplifier to boost the signal. To reduce the power consumption further, a duty-cycling approach is used. The circuit is capable to detect special wake-up packets in the 868 MHz band down to -80 dBm. The power consumption of the circuit was decreased to $14.2 \mu\text{W}$. The reliability and reproducibility of the circuit is a main concern, requiring only commercial off-the-shelf components like general-purpose amplifiers and microcontrollers.

Index Terms—wake-up receiver (WuRx), wireless sensor network (WSN), ultra-low power (ULP), low-noise amplifier, envelope detector, schottky diode, operational amplifier, comparator, fast settling, on-demand, communication

I. INTRODUCTION

The use of batterie-powered and wireless sensor nodes inside large wireless sensor networks (WSNs) is steadily increasing. Powering sensor nodes using small batteries is often mandatory. Decreasing the node's power consumption is necessary. Parameters like latency, transmission range, and sensitivity are major parameters.

Continuous or real-time wireless communication is essential for many applications creating a WSNs. To maintain a continuous wireless communication and ensure low latency, leads to a power consumption greater 10 mW even with modern wireless transceivers. Decreasing the receiving intervals is needed to power a sensor node for a long time with a battery, but increases the latency and response time of the whole WSN.

This work is financially supported by Leipzig University of Applied Sciences by funds of Sächsisches Staatsministerium für Wissenschaft, Kultur und Tourismus.

A wake-up receiver (WuRx) is a special RF receiver that enable the battery-powered sensor node to be in a continuous receiving mode. The mean power consumption of a WuRx is typically kept below $10 \mu\text{W}$ and a very low latency is assured. The wake-up receiver is connected to a second antenna or RF path of the sensor node. Special wake-up packets (WuPts) need to be transmitted by a so-called wake-up transmitter (WuTx) in order to signal the wake-up. Inside the WuPt a address can be introduced, ensuring only one sensor node of the network is woke-up.

WuRx implementations are divided into two categories: application-specific integrated circuit (ASIC)-based WuRx and WuRx implemented using commercial off-the-shelf (COTS) components [1]. This publication will focus on the COTS implementation of WuRx. Fig. 1 shows the typical building blocks of a COTS WuRx.

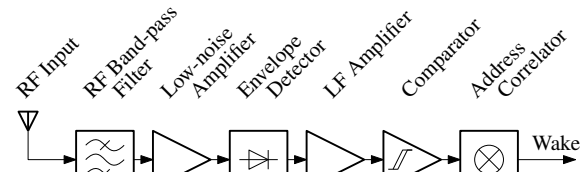


Fig. 1. Building blocks of a typical COTS WuRx with low-noise RF amplifier and passive envelope detector.

The WuRx's input signal is characterized with low amplitude, high noise figure, and various interferences. An RF band-pass filter is used to decrease off-band interferences. To further boost the RF signal and increase the signal-to-noise ratio a low-noise amplifier (LNA) is introduced. A passive envelope detector performs the signal detection and conversion to an LF signal. The LF signal needs to be amplified further in order to be detectable by the following comparator circuit, performing the analog-to-digital conversion. A digital address correlator can be added to implement addressing capabilities of the WuRx and avoid false wake-ups.

II. RELATED WORK

One of the first WuRx designs only utilizing COTS components is [2]. This design was integrated using an envelope detector circuit with a Greinacher voltage double followed by the AS3932 as an integrated amplifier, quantifier and

address correlator. A sensitivity of -52 dBm with a current consumption of only 2.78 μ A was reached.

This design was further improved by [3]. An AS3933 was utilized instead and the envelope detector's LF signal was further amplified by a power-gated operational amplifier (OA) circuit. An ultra-low-power carrier-detection circuit is implemented only enabling the OA when an RF carrier is detected. The sensitivity improved to -60 dBm and the current consumption increased only slightly to 3 μ A.

The publication of [4] introduced the utilization of comparators in order to digitalize the envelope detector's LF signal. The address matching is implemented inside a microcontroller. Also an adaptive reference generator using a low-pass filter on the LF signal was introduced. The performance of different comparator types were investigated. The implementation using the comparator LPV7215 reached a sensitivity -55 dBm while only consuming 1.2 μ W.

The approach presented in [5] introduced a OA circuit between envelope detector and comparator circuit. This allowed to increase the circuit's sensitivity down to -70 dBm while remaining a low current consumption of 580 nA. This is possible due to a very slow data rate of approximately 20 bit/s, resulting into long WuPts and high latency.

The sensitivity of these WuRx implementations is mainly limited by the noise figure of the envelope detector. No implementation using a passive envelope detector were able to reach a sensitivity beyond -60 dBm while maintaining a fast data rate. In order further the increase the WuRx's sensitivity a pre-amplification of the RF signal is needed.

The utilization of a LNA is introduced in [6]. The MAX2643 is able to amplify the RF signal with 17 dBm and a current consumption of 5.3 mA. A high data rate of 250 kbit/s is utilized in order to keep the active times as short as possible. A duty-cycling is introduced with an active time 10 ms every 1 s is used. This results into a average current consumption of 5.7 μ A. A sensitivity of -71 dBm was achieved.

The LNA-based design from [7] utilizes bipolar junction transistor (BJT)-based LNA and LF amplifier. The LNA is able to amplify by 36 dB while only consuming 550 μ A. A comparator circuit is used to digitalize the LF amplifier's output. A special communications schema capable of supporting a duty-cycled receiver is introduced. Low active current consumption of only 1.3 mA and fast settling times enable the WuRx to stay active for only 55 μ s every 32 ms. The average power consumption is 3 μ W while sensitivity is -90 dBm.

III. BUILDING BLOCK ANALYSIS

The following section focuses on the component analysis and selection in order to propose as design of an LNA based WuRx working in the 868 MHz frequency band. Duty-cycling will be utilized in order to decrease the average current consumption. Ensuring low settling times of all components is essential.

A. RF Band-pass Filter

The introduction of an RF band-pass filter is necessary in order to ensure proper WuRx's immunity to interferences from other RF bands. Antenna's, LNA's, and matching circuit's

frequency responses are band-pass shaped, but do not offer a narrow-band response. Introducing a surface acoustic wave (SAW) filter into the WuRx design significantly reduces interferences, but introduce an additional insertion loss.

The utilized SAW filter B39871B3725U410 has a center frequency of 869 MHz, a bandwidth of 2 MHz, and a typical insertion loss of 2.5 dB [8]. This insertion loss directly decreases the WuRx's sensitivity when compared to an ideal system, but the utilization of a SAW filter in a noisy real-live environment is essential.

B. Low-noise Amplifier

This work focuses on the utilization of the MAX2640 COTS LNA [9]. The MAX2640 was selected because of its low current consumption of 3.5 mA and high gain of 14.4 dB. A single-stage design according to Fig. 2 and the datasheet [9] was built up.

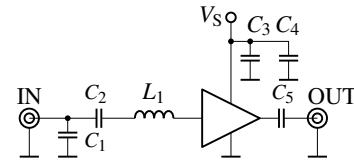


Fig. 2. Schematic of the low-noise amplifier utilizing the MAX2640, based on [9]

With a supply voltage of 3.3 V the LNA showed a current consumption of 3.19 mA. Connecting the test printed circuit board (PCB) to a two-port network analyzer delivered the following S-parameters at 868 MHz: $S_{11} = -20$ dB, $S_{21} = 14$ dB, $S_{12} = -30$ dB, $S_{22} = -15$ dB.

Measuring the settling time of the LNA circuit showed a rather long duration of 7.5 μ s. Decreasing the capacitance of C_1 from 470 pF to 10 pF and matching the circuit, decreases the settling time to 420 ns.

For the proposed WuRx circuit a dual-stage LNA design is used. The total current consumption was measured with 6.7 mA and the S-parameters of the whole circuit are measured as following: $S_{11} = -13.3$ dB, $S_{21} = 27.6$ dB, $S_{12} = -33$ dB, $S_{22} = -15.1$ dB.

C. Impedance Matching and Envelope Detector

Utilizing a Greinacher voltage doubler configuration as an envelope detector circuit is common in recent publications [2]–[5], [7]. Impedance matching is necessary in order to match the 50 Ω output impedance of the LNA to the envelope detector's load impedance. A matching circuit with two lumped components is used, based on the publications [2], [4], [5], [7]. Fig. 3 shows the schematic of the envelope detector.

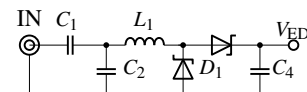


Fig. 3. Schematic of the envelope detector utilizing a Greinacher voltage doubler.

The diode HSMS-2852 from Agilent Technologies is the typical diode used in the envelope detector by many publications [3]–[5], [7]. Because this diode is not any more

provided by the manufacturer, an alternative is needed. The SMS7630-006LF from Skyworks Solution Inc. has nearly identical parameters and the previous investigations were made [10], to ensure that the diode SMS7630 is a good alternative diode.

Below the input power of around -30 dBm the diode behaves according to (1) with V_{ED} the envelope detector output voltage, γ^{OC} the open-circuit voltage sensitivity, and P_{in} the RF input power.

$$V_{ED} = \gamma^{OC} \cdot P_{in} \quad (1)$$

The diode's LF behavior can be modeled as an voltage source with series resistance, so called video resistance R_v . R_v is defined by the diode's series resistance R_s and the diode's junction resistance R_j , see (2) [11, p. 569].

$$R_v = R_s + R_j \quad (2)$$

Voltage sensitivity and video resistance were determined experimental for the setup described in Fig. 3. The envelope detector output voltage was measured for different RF powers. Fig. 4 shows the measurements results.

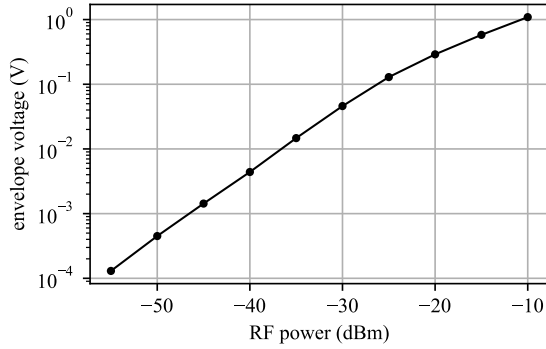


Fig. 4. Results of the voltage sensitivity measurement.

The figure shows clearly the square-law behavior of the envelope detector for input levels lower -30 dBm. The voltage sensitivity resulting into $\gamma^{OC} = 45$ mV/ μ W.

In order to measure the video resistance a load resistor was added. When adding a 10 k Ω resistor the envelope voltage output drops from 44.1 mV to 21.7 mV. The video resistance can be calculated to 11.7 k Ω .

The video resistance forms together with capacitance a low-pass filter. The filter's cut-off frequency has to be chosen accordingly, that RF components are properly removed, but the LF signal is not disturbed. With $C_4 = 10$ pF a cut-off frequency of 1.6 MHz can be estimated according (3).

$$f_C = \frac{1}{2\pi \cdot R_v \cdot C_4} \quad (3)$$

D. LF Amplifier Circuit

Reference [7] utilized a BJT-based amplifier. Because DC-blocking capacitors needed for the BJT amplifier, the LF signal is high-pass filtered. The high-pass filter time constant has to be set accordingly, that the signal is not disturbed and a fast settling time is ensured. Non-inverting OA-based amplifiers do not rely on DC blocking capacitors.

A COTS OA device is selected according current consumption, gain bandwidth product (GBWP) and rail-to-rail capabilities. The TSV6391A was selected and is offering a GBWP of 2 MHz and a current consumption of typically 50 μ A [12].

The input offset voltage of the OA limits the minimal detectable signal. A value of ± 500 μ V at room temperature is given by datasheet [12]. With an envelope detector voltage sensitivity of $\gamma = 45$ mV/ μ W, signal level of only -50 dBm can be detected. That is why a biasing circuit needs to be introduced in order to add a DC voltage to the envelope detector output signal. Fig. 5 shows the utilized amplification circuit with the LF equivalent circuit of the envelope detector.

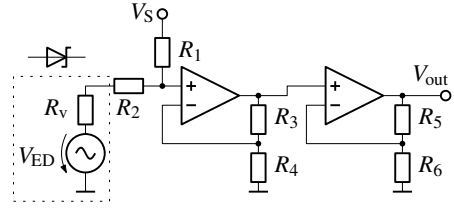


Fig. 5. Schematic of the LF amplifier circuit with envelope detector equivalent circuit, biasing circuit, and dual-stage OA circuit, based on [13].

The envelope detector is replaced by its Thévenin equivalent circuit. The biasing circuit is formed through the voltage divider of R_1 and the series resistance of R_2 and diode's video resistance R_v . The biasing voltage was selected to around 3 mV by setting $V_S = 3.3$ V, $R_1 = 10$ M Ω , and $R_2 = 0$.

A dual-stage amplifier design was utilized in order to increase gain and bandwidth. The feedback resistors R_3 to R_4 were selected to create a amplification factor of 14 per stage, resulting an a total gain of around 200 and a bandwidth of 170 kHz.

E. Comparator Circuit

A COTS comparator needs to be selected according the current consumption and propagation delay. Low propagation delay allowing fast signal transmissions and fast settling times. The input offset voltage and hysteresis of the comparator limits the minimum detectable signal. The TLV3201 is selected because of its low current consumption of 40 μ A and low propagation delay of typically 40 ns [14]. The maximum input offset voltage is given to 5 mV at room temperature.

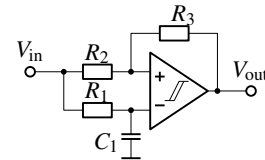


Fig. 6. Schematic of the comparator with external hysteresis and adaptive reference generator, based on [15]

Fig. 6 shows the schematic of the comparator circuit. To compensate the variations in the input offset voltage an external hysteresis circuit is added by the resistors R_2 and R_3 . The hysteresis voltage difference is set to 20 mV.

On the negative input of the comparator a low-pass filter is added, acting like a data slicer. When an symmetrical square-wave signal is applied the capacitor C_1 charges up to half of

the peak-to-peak voltage. The data slicer time constant τ_{DS} is set by the R_1 and C_1 according to (4).

$$\tau_{DS} = R_1 \cdot C_1 \quad (4)$$

Application note [15] recommends the dimensioning $\tau_{DS} = 5 \cdot T_{bit}$ with T_{bit} the bit duration. But large τ_{DS} also increases the settling time of the comparator circuit. That is why τ_{DS} was set to $3.3 \mu\text{s}$, but T_{bit} is $10 \mu\text{s}$. This makes the comparator circuit more susceptible to interferences, but ensures a short settling time.

IV. PERFORMANCE ANALYSIS

The proposed circuit, seen in Fig. 7, was built up. A MSP430G2553 microcontroller is used to control the components' power supplies and perform the address matching [16].

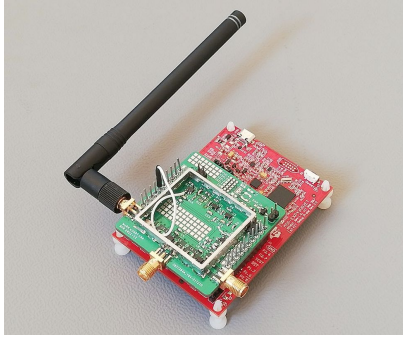


Fig. 7. Prototype PCB with MSP430 Launchpad and 868 MHz antenna.

In order to evaluate the sensitivity of the WuRx packet error rate (PER) measurements are made. Fig. 8 shows the general structure of the PER measurement system, used for the following measurements. A PC is used to control both the frequency generator and a microcontroller interface. The microcontroller is capable to output the LF signal used by the frequency generator to modulate the WuPt. The RF WuPt is connected to the test circuit. An digital output signal is generated by the test circuit on successful WuPt detection and is fed back into the microcontroller. The microcontroller is capable in counting both transmitted and received packets and can estimate the PER. Varying the frequency generator's output power, allows the comparison between different WuRx configurations and setups.

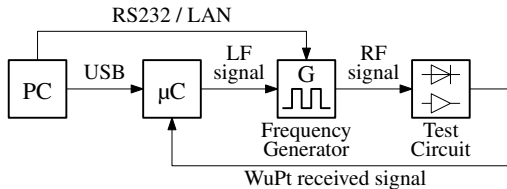


Fig. 8. Block diagram of the PER measurement system.

A. Steady-state Analysis

Fig. 9 shows an oscilloscope measurement with a 50 kHz test signal, modulated onto a 868 MHz carrier with an RF power of -80 dBm . The LF envelope of the test signal can

be seen in the first subplot. The second subplot shows the amplifier output. An offset voltage of 780 mV can be seen, which is created by the bias generator, OAs' input offset voltages and is further amplified. The last subplot shows the comparator output. The successful reconstruction of the test signal can be seen together with several glitches before and after the signal. These glitches occur especially due to the low data slicer time constant.

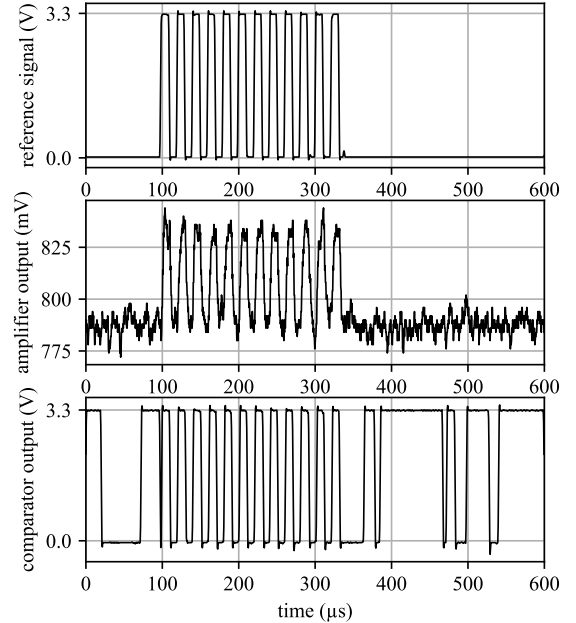


Fig. 9. Steady state oscilloscope measurement with 50 kHz test signal, modulated onto a 868 MHz carrier with an RF power of -80 dBm .

B. Duty-Cycling and Circuit Settling

In order to reduce the average power consumption of the circuit, a duty-cycling approach is introduced. The power supply of the LNA and the LF circuit can be controlled by the MSP430's digital outputs. The WuRx enters the active phase continuously in order to detect incoming WuPts.

During the active phase the WuRx needs to detect the presence of a WuPt and extend the active phase accordingly. Keeping the peek time as short as possible is mandatory to reduce the WuRx's power consumption.

The peek time is strongly dependent on the data slicer time constant τ_{DS} . Using slower τ_{DS} result into a longer settling time, until the square-wave signal is seen on the comparator output. The fastest decision method is to measure and compare the time between two consecutive slopes of the comparator output. This method is also used by [7], but is very sensitive to glitches occurring on the comparator output. Sampling the signal and using multiple signal periods to make this decision would create more reliable results, but would increase the peek time drastically.

The minimal suitable peek time was determined experimentally. Multiple peek times and RF input powers were tested. The number of successful signal detections were counted and the results can be seen in Fig. 10.

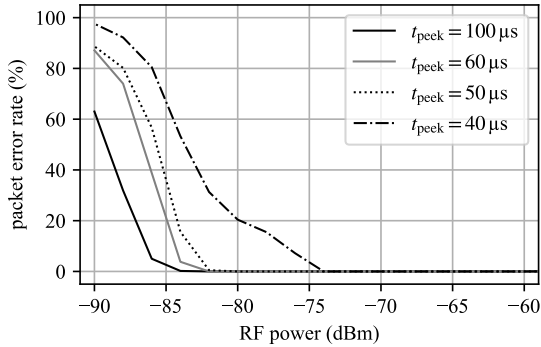


Fig. 10. Measurement of successful detected 50 kHz signal at different input powers and for different active phase duration.

With higher peek time the detection of low-power signals becomes more reliable, but also the number of false-positives increases. Using $t_{\text{peek}} = 40 \mu\text{s}$ results into packet losses starting at -74 dBm . $t_{\text{peek}} = 50 \mu\text{s}$ was selected as suitable for the application.

C. Address Matching

The encoding of an address in the WuPt is essential in order to avoid false wake-ups. Due to duty-cycling the WuRx is randomly started during the transmission of the WuPt. Using pauses within the WuPt is not possible, because the WuRx would not be able to detect the presence of a WuPt and no wake-up will occur. The protocol described in [7], shows such pauses and will result into random packet losses.

The idea proposed in this publication is to use a LF frequency modulation (FM) to encode the wake-up address. Because there is always a signal present and no pauses occur, the WuPt detection during the peek time will not fail. Both 50 kHz and 100 kHz square-wave signals will be used in order to encode binary '1' and '0'. This is done by the microcontroller, measuring continuously the elapsed time between two rising edges of the comparator output.

Fig. 11 shows an example WuPt and the decoder's output signal at an RF power of -75 dBm . The LF reference signal is seen in the first subplot. The second subplot shows the digital output signal of the FM decoding.

The FM signal is selected accordingly, that FM decoding output is a valid universal asynchronous receiver transmitter (UART) signal. This signal is fed back into the microcontroller's UART module. Within the UART interrupt the address matching can be realized. Currently only 8 bit addressing is supported.

D. Timing

Fig. 12 shows the timing diagram for the duty-cycled WuRx communication. t_{peek} is the duration necessary for the WuRx to detect the presence of a WuPt. Due to settling time and data slicer time constant $t_{\text{peek}} = 50 \mu\text{s}$ is used. t_{sleep} is the duration between two active phases of the WuRx. Increasing t_{sleep} will decrease the average power consumption of the WuRx, but will increase the transmission time t_{WuPts} and the WuTx's current consumption. $t_{\text{sleep}} = 100 \text{ ms}$ will be used for the following analysis. t_{WuPt} is the duration of a single WuPt, transmitting

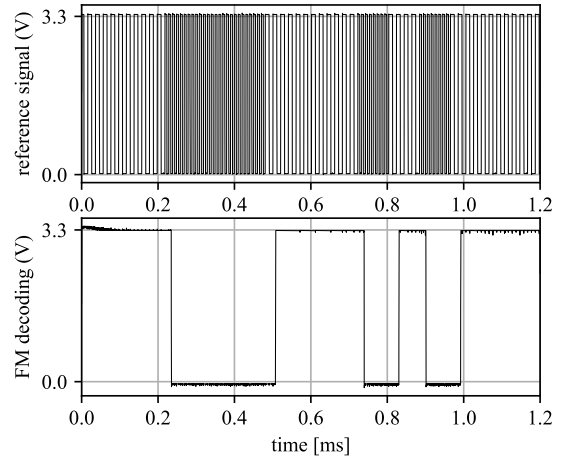


Fig. 11. Oscilloscope measurement of address decoding with 50 kHz and 100 kHz test signal at an RF power of -75 dBm .

the wake-up address once. The FM-demodulated UART signal has a baud rate of 12.5 kbit/s. The 8 bit address together with start bit, stop bit, and padding results into a $t_{\text{WuPt}} = 1.36 \text{ ms}$. The address decoding of the WuRx needs to be at least twice t_{WuPt} to ensure the address is received completely, resulting into $t_{\text{addr}} = 2.8 \text{ ms}$. To ensure that WuRx received the address $t_{\text{WuPts}} > t_{\text{sleep}} + t_{\text{addr}}$, resulting into 76 WuPts being transmitted and $t_{\text{WuPts}} = 103.4 \text{ ms}$.

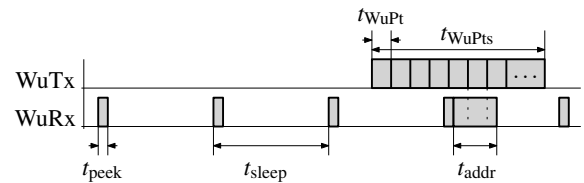


Fig. 12. Timing diagram for duty-cycled WuRx communication.

The programming of the MSP430G2553 microcontroller is done using multiple timers. The first timer uses a ultra-low-power crystal oscillator, generating an interrupt every t_{sleep} , in order to activate the WuRx. During the peek interval a second timer is used in order to measure the duration between two consecutive slopes and generate a timeout signal after t_{peek} . If a valid wake-up signal is detected, the timeout is extended to t_{addr} and the timer is changed to measure the time between two consecutive rising slopes. The FM signal is decoded continuously and fed into the UART module. The UART module generates an interrupt on byte receive. This byte is compared to the 8 bit wake-up address. On successful WuPt reception or timer timeout the WuRx components are turned off again.

E. Sensitivity and Current Consumption

The sensitivity was measured with the PER measurement system. A packet count of $N = 1000$ and a power step size of 2 dB was used to generate the PER curve seen in Fig. 13.

The proposed WuRx shows a PER below 1% down to -80 dBm . Down to -84 dBm WuPt were being detected.

Tab. I shows the current consumption of the proposed WuRx's components. During active phase the current rises

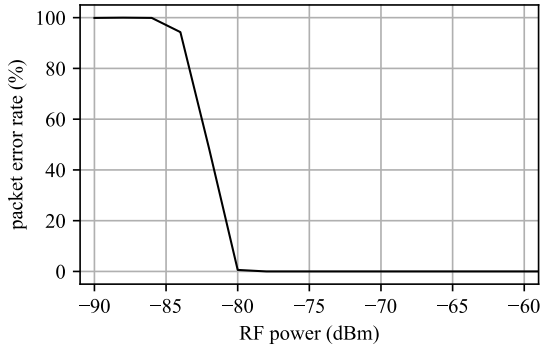


Fig. 13. Measurement of the packet error rate of the proposed wake-up receiver.

to 7.19 mA. During sleep mode all WuRx components are deactivated. Only the microcontroller remains active. With a $t_{\text{peek}} = 50 \mu\text{s}$ and $t_{\text{sleep}} = 100 \text{ms}$ this results into a average current consumption of $\bar{I} = 4.3 \mu\text{A}$ and a average power of $\bar{P} = 14.2 \mu\text{W}$. The current consumption measured on the prototype is slightly increased, because of peek period being extended falsely, due to interferences or noise.

TABLE I
PROPOSED WAKE-UP RECEIVER'S CURRENT CONSUMPTION

	Active	Sleep
Current Draw (μA)		
LNA	6700	0
LF amplifier	120	0
Comparator	40	0
Microcontroller	330	0.7
Total (μA)	7190	0.7
Duration (ms)	0.05	100
Mean Current Draw (μA)	4.3	
Mean Power (μW)	14.3	

V. DISCUSSION

The proposed circuit shows a way to further improve the sensitivity of wake-up receivers (WuRx). Using only commercial off-the-shelf (COTS) components, the circuit and the results can be easily reproduced. Biasing circuit, adaptive threshold generator, and hysteresis ensures that this circuits works reliable, even if component characteristics changes. Exceptionally making the circuit independent of operational amplifier (OA)'s or comparator's input offset voltage. This makes the circuit more reliable compared to proposed circuits of [3]–[5], where circuit's performance strongly varies with component's input offset voltage.

The proposed wake-up packet (WuPt) protocol ensures a reliable WuPt detection during the peek interval. Ensuring no pauses in the WuPt results into a reliable WuPt detection. As shown in Fig. 13, the WuRx is capable to detect the signals above -80dBm , and all 1000 test packets were received.

Sensitivity and power consumption values proposed by [7] were not able to achieve. The circuit's sensitivity is 10 dB less and power consumption is increased by around factor 5. This can mainly explained due to a better performance of the low-noise amplifier (LNA) circuit used by [7]. A gain of 36 dB

instead of 27 dB and a current draw of 550 μA instead of 7 mA is proposed. A supply voltage of 1.8 V instead of 3.3 V is used, resulting in a overall reduced consumption.

Further work has to be made, in order to introducing a buck-converter to efficiently use of the circuit with lower supply voltages. Proper circuit performance down to 2 V has to be ensured. The low frequency (LF) circuit has be further improved in order to remove false-triggers of the comparator and reduced the number of false-wake-ups during the peek interval. Introducing a LNA with higher gain and lower power consumption shall further improve the WuRx's performance.

REFERENCES

- [1] R. Piyare, A. L. Murphy, C. Kiraly, P. Tosato, and D. Brunelli, "Ultra low power wake-up radios: A hardware and networking survey," *IEEE Communications Surveys Tutorials*, vol. 19, no. 4, pp. 2117–2157, 2017.
- [2] G. U. Gamm, M. Sippel, M. Kostic, and L. M. Reindl, "Low power wake-up receiver for wireless sensor nodes," in *2010 Sixth International Conference on Intelligent Sensors, Sensor Networks and Information Processing*, 2010, pp. 121–126.
- [3] S. Bdiri and F. Derbel, "An ultra-low power wake-up receiver for real-time constrained wireless sensor networks," in *Proceedings SENSOR 2015*, 05 2015.
- [4] M. Magno, V. Jelicic, B. Srbinovski, V. Bilas, E. Popovici, and L. Benini, "Design, implementation, and performance evaluation of a flexible low-latency nanowatt wake-up radio receiver," *IEEE Transactions on Industrial Informatics*, vol. 12, no. 2, pp. 633–644, 2016.
- [5] G. Kazdaridis, N. Sidiropoulos, I. Zografopoulos, and T. Korakis, "eWake: A novel architecture for semi-active wake-up radios attaining ultra-high sensitivity at extremely-low consumption," 2021.
- [6] F. Pflaum, R. Weigel, and A. Koelpin, "Ultra-low-power sensor node with wake-up-functionality for smart-sensor-applications," in *2018 IEEE Topical Conference on Wireless Sensors and Sensor Networks (WiSNet)*, 2018, pp. 107–110.
- [7] S. Bdiri, F. Derbel, and O. Kanoun, "A tuned-rf duty-cycled wake-up receiver with -90 dbm sensitivity," *Sensors*, vol. 18, no. 1, 2018. [Online]. Available: <https://www.mdpi.com/1424-8220/18/1/86>
- [8] RF360 Europe GmbH, "SAW RF filter - B39871B3725U410," 2019, datasheet.
- [9] Maxim Integrated, "300MHz to 2500MHz SiGe ultra-low-noise amplifiers," Feb. 2015, datasheet.
- [10] R. Fromm, L. Schott, and F. Derbel, "An efficient low-power wake-up receiver architecture for power saving for transmitter and receiver communications," in *Proceedings of the 10th International Conference on Sensor Networks - SENSORNETS*, INSTICC. SciTePress, 2021, pp. 61–68.
- [11] I. Bahl and P. Bhartia, *Microwave Solid State Circuit Design*. New York: Wiley, 2003.
- [12] STMicroelectronics NV, "TSV6390, TSV6390A, TSV6391, TSV6391A - micropower (60 μA), wide bandwidth (2.4 MHz) CMOS operational amplifiers," Dec. 2015, datasheet.
- [13] Texas Instruments, "Single-supply op amp design techniques," Mar. 2001, application report.
- [14] —, "TLV320x 40-ns, microPOWER, push-pull output comparators," Dec. 2016, datasheet.
- [15] Maxim Integrated, "Data slicing techniques for UHF ASK receivers," Dec. 2005, application note 3671.
- [16] Texas Instruments, "MSP430G2x53, MSP430G2x13 - Mixed Signal Microcontroller," May 2013, datasheet.